future internet

MDPI

Article

User Association Performance Trade-Offs in Integrated RF/mmWave/THz Communications

Noha Hassan [1,*], Xavier Fernando [1], Isaac Woungang [2] and Alagan Anpalagan [1]

[1] Department of Electrical, Computer and Biomedical Engineering, Toronto Metropolitan University, Toronto, OT 66777, Canada; fernando@torontomu.ca (X.F.); alagan@ee.torontomu.ca (A.A.)
[2] Department of Computer Science, Toronto Metropolitan University, Toronto, OT 66777, Canada; iwoungan@torontomu.ca
* Correspondence: noha.hassan@torontomu.ca

Abstract: In combination with the expected traffic avalanche foreseen for the next decade, solutions supporting energy-efficient, scalable and flexible network operations are essential. Considering the myriad of user case requirements, THz and mmW bands will play key roles in 6G networks. While mmW is known for short-rate LOS connections, THz transmission is subjected to even severe propagation losses, resulting in very short-range connections. In this context, we evaluate a dynamic multi-band user association algorithm to optimize connectivity in coexisting RF/mmW/THz networks. The algorithm periodically calculates association scores for each user–base station pair based on real-time channel conditions across bands, accounting for factors like signal strength, link blockage risk and noise. It then reassociates users in batches to balance loads while considering user priorities and network conditions. We simulate the algorithm's performance within a realistic propagation model, where high path loss, molecular absorption, blockage, and narrow beam widths contribute to lower coverage at higher frequencies. Results demonstrate the algorithm's ability to efficiently utilize network resources across diverse operating environments. In addition, our results show that the choice of frequency band depends on the specific requirements of the application, the environment, and the trade-offs between coverage distance, capacity, and interference conditions.

Keywords: coverage probability; SINR distribution; user association; millimeter wave; terahertz; 6G wireless networks

Citation: Hassan, N.; Fernando, X.; Woungang, I.; Anpalagan, A. User Association Performance Trade-Offs in Integrated RF/mmWave/THz Communications. *Future Internet* **2023**, *15*, 376. https://doi.org/10.3390/fi15120376

Academic Editor: Symeon Papavassiliou

Received: 9 October 2023
Revised: 20 November 2023
Accepted: 22 November 2023
Published: 24 November 2023

1. Introduction

Sixth-generation wireless networks are expected to support a wide range of emerging applications, including augmented reality, tactile Internet, wireless brain interfaces, connected robotic systems, and holographic telepresence. To enable these applications, 6G will require extremely high data rates with low latency and high reliability [1].

As the current sub-6 GHz spectrum is becoming crowded and cannot meet the growing demands, mmW and THz frequency bands have been proposed to provide the needed additional spectrum and higher data rates [2,3]. Broadly, RF includes all frequencies from around 9 kHz to 300 GHz, encompassing both microwaves and lower frequencies. This is the broadest definition. More specifically, RF is often defined as 3 kHz to 30 GHz, with microwaves considered separately from 30 GHz to 300 GHz. For cellular communications (Telecom), "RF bands" commonly refers to frequencies below 6 GHz (aka sub-6 GHz), which includes licensed LTE and 5G bands.

mmW and THz technologies are poised to enable key capabilities that will drive many emerging applications. Specifically, the use of higher frequencies allows for the highly accurate estimation of wireless channel characteristics and device-positioning parameters. This level of precision will underpin the delivery of location-aware services that have become increasingly prevalent. In addition, the massive bandwidths available at mmW

and THz frequencies facilitate multi-gigabit data rates and wireless connections with ultra-low latency. Together, the abilities to accurately localize, deliver high data throughput, and minimize latency will be crucial for applications such as augmented/virtual reality, autonomous systems, telemedicine, and industrial automation that require real-time, context-aware wireless connectivity. mmW and THz communications are widely seen as essential technologies for fully realizing these next-generation applications [4,5].

The International Telecommunication Union (ITU) defines mmW frequencies as ranging from 30 GHz to 300 GHz. This is a broad definition encompassing the whole millimeter wavelength range, which offers multi gigabit data rates due to the large available bandwidth. For 5G cellular applications (also defined by the US Federal Communications Commission), mmW is often referred to more narrowly as frequencies between 24 GHz and 100 GHz. This captures the mid-band mmW frequencies being used for 5G. Currently, in Canada, 5G mmW describes radio signals in three frequencies: 26, 28, and 38 GHz. However, mmW signals have high attenuation and cannot penetrate solid materials and walls. This leads to blockage issues and requires LOS or highly directional transmissions [6]. THz bands (0.3 to 10 THz) or wavelengths between 1 mm and 100 µm provide even higher data rates and capacity, enabling terabit wireless applications. For communication applications, some sources define THz as frequencies above 100 GHz, i.e., bordering the upper end of mmWave bands. This definition includes lower THz frequencies. The term "THz gap" is sometimes used to refer specifically to frequencies between 0.3 and 3 THz [7], reflecting the challenges of this mid-band range. Some sources define THz communication beginning at wavelengths shorter than 1 mm, or frequencies above 1 THz. This excludes lower THz frequencies. However, it faces challenges due to high atmospheric and molecular absorption losses, strong signal attenuation, and limited propagation range [8,9].

To compensate for the high propagation losses at THz/mmW frequencies, 6G networks will utilize "ultra-massive MIMO" techniques with large antenna arrays embedded in surfaces, dense arrays of plasma nano-antennas that can be integrated into walls and objects to provide highly directional beamforming gains. The integration of satellite, optical, and molecular communications with intelligent reflecting surfaces will help provide a truly ubiquitous connectivity envisioned for 6G networks [10,11].

Although THz and mmW bands offer much larger bandwidths compared to RF, the impact of interference and noise becomes more critical with the increased bandwidth, and practical implementation challenges arise [9]. Therefore, the greatly expanded spectrum at the mmW and THz frequencies will be key enablers for 6G applications that will require terabit data rates and low latency. However, overcoming challenges like blockage, absorption losses, and limited range will require innovative user association techniques [12].

The seamless integration of high- and low-frequency bands' cells imposes a number of challenges since different BSs will have different transmission powers, coverage areas and data rate capabilities and need to cater to different types of UEs. Therefore, developing a proper UE-BS association algorithm for diverse 6G networks is a tough task [13]. Such an appropriate algorithm shall not only improve the QoS performance for each UE, but shall also ensure fairness for both UEs and BSs [14].

UE association methods have been widely used in cellular networks to optimize network performance by selecting the best serving cell or frequency band for each UE. Traditional user association strategies that simply maximize the SINR ratio [15] cannot be applied here. This will lead to imbalanced load distributions across frequency bands and cells since the UEs tend to associate with the lowest-frequency (RF) band BSs, which would have better better SINR due to the better propagation characteristics and higher transmit powers.

This imbalanced load distribution will result in the inefficient utilization of the network's resources, where RF band cells would be overloaded, while the THz/mmW band would be underutilized. To achieve an equitable load distribution and efficient resource utilization, more sophisticated user association strategies that go beyond simply maximiz-

ing the received signal strength are needed. Individual user association, just considering only one band at a time, will not yield globally optimized results.

In this paper, we propose a unified multi-band user association algorithm to optimize the user throughput and satisfaction in next-generation 6G wireless networks considering all three bands. We consider three types of user cases: enhanced broadband, low latency and high-reliability connections, each with different QOS requirements. Our proposed algorithm aims to associate each user with the best available BS using the best possible band considering real-time channel conditions across bands, while accounting for user preferences. It considers key factors, such as signal strength and link blockage probability that vary significantly by frequency. The algorithm recomputes user–BS scores periodically and reassociates users in batches to dynamically balance loads. Through comprehensive system-level simulations under realistic scenarios, we demonstrate the effectiveness of our approach in efficiently utilizing network resources across diverse operating conditions. The multi-band association technique paves the way for optimized performance in emerging multi-band wireless networks.

2. Related Work

User association methods have been widely used in cellular networks to optimize network performance by selecting the best serving cell or frequency band for each user. Traditional user association schemes utilize parameters like received signal strength (like max-SINR [15]) and channel conditions to associate users with the cell or band that provides the highest SNR or SINR. However, such approaches often lead to load imbalance issues and inefficient resource utilization, potentially causing severe impairments in certain links.

To address these issues, some authors have introduced biased algorithms, such as the CRE algorithm [16,17], which artificially enhances the signal strength of weaker BSs by applying a certain bias factor. While this approach has shown promise in increasing system throughput and capacity, its performance is contingent upon the choice of the bias factor, which poses challenges in determining the optimal value. As a result, the performance of less powerful BSs may be negatively affected.

Another interference avoidance method is resource partitioning, called time domain eICIC [18,19]. eICIC uses the muting/coordination of resources, where it coordinates resource allocation between overlapping macro and small cells. Macro cells can mute some subframes, allowing small cells to reuse those resources. This reduces interference from macrocells to small cell users without changing the TX power levels. While eICIC is effective for same-RAT HetNets, applying its interference coordination approach across fundamentally different radio technologies with varying capabilities will be very complex.

Some works consider both the SINR and existing load (like our previous algorithms [20,21]. While this balances the SINR and load distribution better than max-SINR, this still considers absolute SINR values without normalization across bands. This would skew results towards the RF band.

Even incorporating blockage probability [22] instead of raw SINR may still favor the RF band since its blockage probability of RF is effectively zero. Normalization or other techniques are needed to overcome this bias.

More recent work has explored optimization-based user association methods that aim to maximize network-wide utility or fairness metrics while balancing the load across cells and frequency bands [23–25]. Such schemes incorporate factors like network congestion, user rates, cell capacities, load variances, cell loads, bandwidths, and handover costs into the optimization objective, which can enable load balancing across the network to improve service rates for all UEs. For example, some studies [26–29] have formulated user association as a mixed-integer program that jointly optimizes user–cell associations and resource allocation to maximize the sum rate of the network. However, these algorithms often result in complex integer programs that are difficult to solve in real time.

Other works have used game-theoretic approaches [30,31], where each user associates with the cell or band that maximizes its own utility while considering the impact on

other users. Game theoretic approaches require iterative signaling between users and the network, increasing the signaling overhead. They also assume rational users who would compromise their own utility.

Machine learning methods such as reinforcement learning [32–34] have also been explored to dynamically associate users based on real-time network conditions. These self-organizing techniques can address issues like non-convexity and complexity that arise in optimization formulations. However, reinforcement learning approaches generally require large amounts of data and high-dimensional state and action spaces, and may suffer from poor reproducibility and explainability.

In summary, existing algorithms either do not provide fair load distribution, skew results towards RF bands due to higher intrinsic SINR/lower blockage probability, or have issues with high complexity, signaling overhead or data requirements as shown in Table 1. A low-complexity, efficient algorithm is needed to avoid these limitations.

Table 1. Summary of previous user association methods.

Method	Year	Key Advantages	Key Limitations	Suitability for mmW/THz
SINR-based	2012	Simple implementation; associates users to BS with strongest signal	Does not consider load balancing or multi-band characteristics	Not suitable due to variability in bands
Biased algorithms	2015–2017	Increased capacity and throughput	Optimal bias factor difficult to determine	Marginally improves performance
eICIC	2013–2017	Reduces interference in HetNets	Complex to apply across technologies	Complexity limits applicability
Load-aware	2019–2020	Balances SINR and load	Favors RF band due to higher intrinsic SINR	Better than SINR but still biased
Blockage-aware	2021	Considers propagation effects	Improved but bias toward RF remains	
Optimization	2018–2023	Maximizes network utility	Complex formulations, high complexity	High complexity limits real-time use
Game theory	2020–2021	Models user self-interest	High signaling overhead, assumptions	Signaling overhead challenging
Reinforcement learning	2017–2021	Adapts dynamically	High computational cost; requires extensive training; poor explainability	Applicable but data/complexity concerns

3. System Model

We consider a system with BSs that are subdivided into three BS types: (1) RF (k_1), where $k_1 \in \{1, 2, 3, ...K_1\}$; (2) mmW ($k_2$); and (3) THz ($k_3$). These BS are geographically distributed according to a homogeneous Poisson point process (PPP) [35], ϕ_k of density λ_k. The BS transmission power is P_{T_k}, and the minimum allowed distance between any two BSs is d_{min}. Each BS serves U number of single-antenna users with the same transmit power P_u. Note that λ_u is the UE density.

Each BS and user is equipped with an antenna array that can form directional beams via beamforming. Beamforming vectors define the direction and beamwidth of each link. Beamwidths vary by frequency based on array size. Incorporating directional beamforming provides a realistic 5G/6G channel model by capturing aspects such as gain/interference variations due to beams, multi-user MIMO through multi-beam transmission, and 3D propagation characteristics.

For the RF band, we model the interference-limited coverage probability. Also, UEs, interferers, and blockages are distributed according to a PPP. Blockages are modeled as rectangles with a defined length and width. Links can be either LOS or NLOS depending on whether they are blocked. For the THz system, molecular absorption loss and exponential path loss are used to model propagation loss. System losses are also defined. The total noise consists of thermal noise and molecular noise.

For the BS-UE links, we consider a block-fading channel model with large- and small-scale Rayleigh fading [36,37]. Large-scale fading depends on the distance and path loss, which vary by frequency band. The multi-path small-scale fading coefficients are assumed to be Rayleigh distributed.

The system is assumed to be open access, where there is no restriction on the association of UEs to a certain BS.

OFCDM is considered for the BS to UE links (access downlinks), as it outperforms OFDM for high-speed communications. The system uses coded orthogonal channels, where N_b is the number of transmitted bits (each with bit energy E_b). Also, N and F are the spreading factors in time and frequency domains, respectively. The transmitted signal is spread with Pseudo Noise (PN) sequences in the time domain with chip energy E_c and chip duration T_c, where

$$E_c = E_b/(N \times F) \tag{1}$$

3.1. SINR Calculation

SINR is estimated using frequency-specific path loss and noise models. For the RF band, the path loss is modeled using a logarithmic distance-based model (COST 231) [38]. For mmWave bands, additional penetration losses are considered based on common building materials measured as in TR38.901 [39]. For THz bands, molecular absorption losses are characterized using coefficients from propagation measurements in varying atmospheric compositions [40,41].

The SINR model for RF communication can be given as follows [42]:

$$SINR^{RF} = \frac{P_{T_0} G_T G_R A d_0^{-\alpha} h_0}{N_0 + A \sum_{i=1}^{N} P_{T_i} G_i d_i^{-\alpha} h_i} \tag{2}$$

where $A = \frac{c^2}{16\pi^2 f^2}$, f is frequency, c is light speed, G_T and G_R are the directional gains of the transmitting and receiving beams, α is the attenuation coefficient, d is the distance from the transmitter to the receiver, P_{T_0} is the transmitted power, N_0 is the Johnson–Nyquist noise, N is the number of interferes, G_i is the interfering link beam gain that is reduced if beams do not align well, and h_0 is the small-scale fading gain.

SINR for mmW LOS BSs communication is calculated as [43,44]:

$$SINR_{LOS}^{mmW} = \frac{P_{T_0} G_T G_R A_0 d_0^{-\alpha} B_{mm}}{N_0 + \sum_{i=1}^{N} P_{T_i} G_i A_i d_i^{-\alpha}} \tag{3}$$

SINR for mmW NLOS BSs communication is calculated as:

$$SINR_{NLOS}^{mmW} = \frac{P_{T_0} G_T G_R A (d_{10} + d_{20})^{-\alpha} B_{mm}}{N_0 + A \sum_{i=1}^{N_{rays}} \sum_{i=1}^{N} P_{T_i} G_i (d_{1_i} + d_{2_i})^{-\alpha}} \tag{4}$$

The path loss received from NLOS components communication considers the presence of scatters between the transmitter and the receiver [43], where d_1 is the distance from the transmitter to the scatterer, d_2 is the distance from the scatterer to the receiver, N_{rays} is the number of NLOS rays, and B_{mm} represents the blockage probability, which is calculated analytically as:

$$B_{mm} = e^{-\frac{2\pi\lambda_b \rho}{\gamma}} \tag{5}$$

Here, λ_b is the density of blockages, ρ is the typical width of blockages, and γ is the viewing angle. The blockage calculation considers beam directions—a blockage may only partially obstruct a directional link.

SINR for THz LOS communication is calculated as [43,44]:

$$SINR_{LOS}^{THz} = \frac{P_{T_0} G_T G_R A d_0^{-\alpha} e^{-K d_0} B_{mm}}{N_0 + A \sum_{i=1}^{N} P_{T_i} G_i d_i^{-\alpha}} \tag{6}$$

where K is the absorption coefficient of the medium, and N_0 is the Johnson–Nyquist noise plus the molecular noise equal to $N_0 = K_B T + P_{T_0} A_0 d_0^{-2}(1 - e^{-} K d_0)$, considering K_B as the Boltzman constant and T as the temperature.

SINR for Tera Hertz NLOS communication is calculated as:

$$SINR_{NLOS}^{THz} = \frac{P_{T_0} G_T G_R A (d_{1_0} + d_{2_0})^{-\alpha} e^{-K(d_{1_0}+d_{2_0})} R(f) B_{mm}}{N_0 + A \sum_{i=1}^{N_{rays}} \sum_{i=1}^{N} P_{T_i} G_i (d_{1_0} + d_{2_i})^{-\alpha}} \quad (7)$$

where $R(f)$ is the reflection coefficient of a rough surface equal to the Rayleigh roughness factor times the smooth surface reflection coefficient derived from the Fresnel equations. This is given by the expression [45]:

$$R(f) = e^{-} \frac{2\cos(\theta_1)}{\sqrt{\mu_r \varepsilon_r - 1}} \times e^{-} \frac{8\pi f \sigma \cos(\theta_1)}{c \times d_2} \quad (8)$$

where θ_1 is the angle of incidence, and σ is the rough surface height standard deviation, commonly assumed to be Gaussian distributed.

Based on the equations provided, the total SINR would be a weighted sum of the LOS and NLOS SINR:

$$SINR_{total} = w_{LOS} * SINR_{LOS} + w_{NLOS} * SINR_{NLOS} \quad (9)$$

where w_{LOS} and w_{NLOS} are the weights for the LOS and NLOS SINR, representing their relative importance or reliability $w_{LOS} + w_{NLOS} = 1$.

LOS signal tends to be more reliable, so typically $w_{LOS} > w_{NLOS}$.

3.2. Beamforming Model

Directional beamforming is implemented at BSs and UEs using uniform linear antenna arrays. The beamforming vectors define the direction and beamwidth of each link.

3.2.1. Beam Management

Beam training and tracking ensure proper alignment between the transmitter and receiver beams.

- Training: At association/handover, beams are aligned through channel estimation and feedback over τ seconds. To calculate the training overhead, let τ be the beam training time, T be the data transmission time per beam, and the total overhead per beam = $\tau + T$.
  The effective rate reduces to:

$$R_eff = (1 - \tau/T)R \quad (10)$$

  where R_eff is the effective achievable rate accounting for the beam training overhead (bps), and R is the max achievable rate without the beam training overhead (bps).
- Tracking: The beam tracking mechanism accounts for the continuous adaptation of beams to changing channel conditions over time. Due to channel variations between BSs and UEs, the optimal beamforming weights need periodic adjustment to maintain high signal quality. The model captures this by estimating the channel state every T_b seconds to perform beam tracking. However, there is an inherent tracking error that causes an angular offset. Beams may not be perfectly aligned due to factors like mobility; this misalignment leads to reductions in the beamforming gain achieved.
  The beamforming gain equals:

$$G = G_{max} \times e^{\left(-\frac{\theta}{\theta_{3dB}}\right)} \quad (11)$$

where θ is the offset between the adapted beam and the true optimal beam orientation, which follows a Gaussian distribution, θ_{3dB} represents the half-power beamwidth, and G_{max} is the maximum possible beamforming gain attained with perfect beam alignment. The lower gain resulting from tracking errors then translates to an additional rate loss for each user. By incorporating beam tracking dynamics, the model realistically reflects the time-varying nature of wireless channels and associated impacts on beamformed transmissions.

3.2.2. Beam Scanning:

The beam scanning mechanism models the periodic beam scanning performed by the base station to enable user discovery and handovers between beams/BSs. During the scanning process, the BS sequentially surveys each of the S sectors in its coverage area. For each sector, there is a time t_{train} required to train the beam in that direction. Once the beam training is complete, there is also a detection time t_{det} needed to detect the pilot signal from any user equipment currently in that sector. The total time spent scanning each individual sector is therefore given by $t_{train} + t_{det}$. As the BS must sequentially scan through all S sectors, the overall latency experienced by a UE to associate with the network through the beam scanning process is $S * (t_{train} + t_{det})$. This model captures the overhead incurred during the initial network access and handovers between beams or cells.

3.2.3. Beamwidth Adjustment:

Array antennas dynamically adjust beamwidths to balance coverage vs. interference footprints.

The dynamic beamwidth adjustment mechanism allows the beamwidth to be controlled via a parameter β, where $0 < \beta \leq 1$. The nominal beamwidth of each beam is defined as $BW_{nominal}$. The actual beamwidth formed is then given by $BW_{actual} = \beta * BW_{nominal}$. A smaller value of β results in a narrower actual beamwidth. This affects the coverage area and beamforming gain differently. The coverage area provided by a beam is directly proportional to the actual beamwidth. Meanwhile, the beamforming gain is inversely proportional to the actual beamwidth. Therefore, selecting a smaller β increases the beamforming gain but reduces the coverage area serviced by that beam. This allows a tradeoff between the coverage and gain that can be exploited based on dynamic network conditions.

4. Coverage Probability Analysis

To calculate the coverage probability for a given scenario with three types of users and three types of base stations, let us consider the subscript u and k for any user and base station indices in general and z for the subcarrier index.

The coverage probability for a given user u associated with base station k and served by subcarrier z, denoted as (the same equation is applicable to all three bands) $P_c(\gamma_{k,u}^{(z)})$, can be expressed as [20]:

$$P_c(\gamma_{k,u}^{(z)}) = \frac{\sqrt{\sigma}}{2} N^2 E_c^2 \lambda_k \int_{\mathbb{R}^2} e^{\left[\frac{\left(\frac{\zeta_k^2}{P_{T_k}^2 |d_{k,u}|^{-2\alpha}} \right) \sigma^2}{2} - \left(\mu + \sigma^2 \right) \left(\frac{\zeta_k}{P_{T_k} |d_{k,u}|^{-\alpha}} \right) \right]} \mathrm{d}(\mathbf{d_{k,u}}) \quad (12)$$

where λ_k is the density of base station k (BSs per unit area), E_c^2 is the signal power considering the PN sequence, ζ_k is the SINR threshold for coverage for user u associated with BS k, P_{T_k} is the transmit power of BS k, μ is the mean of the interference distribution, σ^2 is the variance of the interference distribution, R is the cell radius, $|d_{k,u}|$ is the distance from the BS k to the user u, and α is the path loss exponent. Since there are three different types of users (radio frequency, millimeter wave, and terahertz), each with its own SINR threshold and path loss exponent, we need to calculate the coverage probability separately for each user type and then combine the results.

Let us denote the three types of users as u_1 (radio frequency), u_2 (millimeter wave), and u_3 (terahertz), and their corresponding base stations as k_1, k_2, and k_3, respectively.

The total coverage probability, denoted as $P_{c,\text{total}}$, is the probability that any of the three users achieves the required SINR threshold. Therefore, it can be expressed as:

$$P_{c,\text{total}} = 1 - \prod_{i=1}^{3}(1 - P_c(\gamma_{k_i,u_i}^{(z)})) \tag{13}$$

Here, $P_c(\gamma_{k_i,u_i}^{(z)})$ represents the coverage probability for user u_i associated with base station k_i and served by subcarrier z. The expression above accounts for the fact that the overall coverage probability is determined by the probability that at least one of the three users achieves coverage.

To evaluate $P_{c,\text{total}}$, we need to calculate the individual coverage probabilities $P_c(\gamma_{k_i,u_i}^{(z)})$ for each user type based on their respective SINR thresholds, path loss exponents, and other parameters.

The coverage probability for a randomly located UE can be written as:

$$P_c = \mathbb{P}(\bigcup_{k\in K} \max_{d_k\in\phi_k} \gamma_k > \zeta_k) \tag{14}$$

where γ_k is the SINR from the kth BS, ζ_k is the SINR threshold, and ϕ_k is the set of BSs in the kth tier.

Using the Law of Total Probability and Union Bound, we can rewrite the coverage probability for an RF user as:

$$P_c = \sum_{k\in K} \lambda_k N^2 E_c^2 \int_{\mathbb{R}^2} \mathbb{P}(\gamma_k > \zeta_k) d(d_k) \tag{15}$$

where λ_k is the density of the BSs in each band, $\ell(\mathbf{d_{k,u}}) = \|\mathbf{d_{k,u}}\|^{-\alpha}$, $\mathrm{d}(\cdot)$ is the derivative operator, and d_k is the measure of the distance from the UE to the serving BS.

The probability term can be expressed using the Laplace transform of interference $\mathcal{L}_I(.)$ as:

$$\mathbb{P}(\gamma_k > \zeta_k) = \mathcal{L}_I\left(\frac{\zeta_k P_{T_k}\ell(d_k)}{\sigma_n^2}\right) e^{-\frac{\zeta_k\sigma_n^2}{P_{T_k}\ell(d_k)}} \tag{16}$$

Assuming interference is Gaussian distributed, with μ and σ^2 being the mean and variance of the Gaussian distribution, respectively, the Laplace transform can be calculated as:

$$\mathcal{L}_I(s) = \frac{\sqrt{\sigma}}{2} e^{\frac{s^2\sigma^2}{2} - s(\mu+\sigma^2)} \tag{17}$$

Substituting this back into the coverage probability expression, we obtain (12), which is typically the coverage probability equation for the RF band. This equation can be solved analytically.

For mmW and THz systems, blockages are a significant factor due to the higher frequency of waves. These blockages can be modeled by incorporating a blocking probability. The modified coverage probability for the millimeter wave user, denoted as $P_{c,\text{mm}}$, can be expressed as

$$P_{c,\text{mm}} = (1 - B_{mm}) P_c(\gamma_{k_{\text{mm}},u_{\text{mm}}}^{(z)}) \tag{18}$$

Here, $P_c(\gamma_{k_{\text{mm}},u_{\text{mm}}}^{(z)})$ is the coverage probability for the millimeter wave user, and $(1 - B_{\text{mm}})$ accounts for the probability of the user not being blocked. In more detail, the equation is expressed as follows:

$$P_{c,mm} = (1 - B_{mm}) \frac{\sqrt{\sigma}}{2} N_{mm}^2 E_{c,mm}^2 \sum_{k\in K_{mm}} \lambda_{k,mm} \int_{\mathbb{R}^2} e^{[\ldots]} d(d_{k,mm}) \tag{19}$$

For the THz user, we need to consider molecular absorption losses and Lambertian scattering loss, which can significantly impact the signal strength. The coverage probability will be:

$$P_{c,THz} = e^{-\kappa_a d_{k,THz}} G_{THz}(1 - B_{mm}) \frac{\sqrt{\sigma}}{2} N_{THz}^2 E_{c,THz}^2 \sum_{k \in K_{THz}} \lambda_{k,THz} \int [...] d(d_{k,THz}) \quad (20)$$

where κ_a is the absorption coefficient, $d_{k,THz}$ is the distance to the serving THz BS, and G_{THz} is the antenna gain due to the Lambertian scattering loss given by:

$$G_{THz} = \frac{n+1}{2\pi} cos^n(\theta) \quad (21)$$

where n is the Lambertian emission order, and θ is the irradiation angle.

This probability depends on the specific environmental conditions and absorption properties of the medium the signal travels through.

5. Algorithm Description

Our algorithm aims to distribute users evenly among base stations to balance the network load among all three frequency bands.

Any user association algorithm that is based on simply taking the max SINR would not provide a fair load distribution. It skews associations towards the RF band, which often has higher SINR. It also does not consider load balancing between base stations, and it is prone to ping-pong handovers, as SINR can fluctuate.

Combined SINR/Load Balancing user association algorithms take into account both the channel conditions (SINR) and queue length (BS load) when making user association decisions. This allows it to find a good balance between SINR and load distribution.

However, they still consider the absolute SINR values directly, without any normalization across bands. This ends up skewing the results, as it does not properly address the bias towards RF bands inherent in the raw SINR values. Normalization or randomized selection is needed.

In addition, mmW and THz bands are affected by blockage, but the RF band is not. If we prioritize users based on the future expected blockage probability, since RF has no blockage, the results will be skewed too.

The algorithm may still favor associating users to RF BSs if the blockage probability is not considered for RF.

To address this, one approach is the following:

- Incorporate a blockage probability model for each band (mmW/THz higher than RF).
- Calculate an expected SINR value that factors in the blockage probability.

  For example:
  Expected SINR = Raw SINR $\times$ (1 $-$ Blockage Probability)

- Use the expected SINR values (instead of raw SINR) when calculating metrics.

However, even with incorporating an expected SINR that factors in the blockage probability, the results may still skew towards RF associations since the blockage probability for RF is effectively zero.

A better algorithm would need to normalize/equalize the SINR across bands in a more fundamental way before associating users. A few approaches:

1. Normalize raw SINR values across bands to a common scale (e.g., 0–1) before any metric calculation.
2. Calculate a score for each user–BS pair that considers both the SINR and blockage risk, rather than just the expected SINR. For example: Score = NormSINR/(1 + BlockageRisk)
3. Assign users randomly to BSs in different bands based on weighted probabilities, where weights are adjusted based on NormSINR and BlockageRisk.

4. Explicitly require a minimum number/percentage of users to associate to each band to enforce balanced associations.
5. Introduce an additional "band preference" or reward factor for mmW/THz that compensates for their higher risk, to make the bands more competitive against RF.

Here, the key challenge is finding a way to equalize the impact of SINR and reliability across bands before associating users, rather than relying on the expected SINR alone. Normalization and introducing separate scoring factors seems needed.

We need to bear in mind that not all users in 6G systems have the same needs—some prioritize high data rates, others reliability, latency, etc. This affects which frequency bands may be preferable for different users. Also, this exploits multi-band diversity and dynamically optimizes associations under different channel conditions.

1. The algorithm should categorize users based on their profile/preferences:
   - High-data-rate users prefer THz.
   - Low-latency users prefer mmWave.
   - Users requiring reliable connectivity prefer RF.
2. Then, prioritize associating users to bands that best match their needs:
   - Higher weight/preference given to preferred bands in scoring.
   - Explicit cap on preferred band's user limits.
3. User profiling could consider:
   - Application types (video, voice, and IoT sensors).
   - Device capabilities.
   - Service-level agreements.
   - The profile is learned/updated over time based on user behavior.

Here are the steps to implement the multi-band user association algorithm based on the problem statement:

1. Collect the network parameters:
   - User profiles, positions, and applications.
   - Base station positions and supported frequency bands.
   - Blockage probability models per band.
2. Categorize users based on profile:
   - High data, low latency, reliability, etc. Users are categorized into profiles like high-data, low-latency, etc., based on their usage preferences. This forms association priorities.
3. Calculate band metrics:
   - Raw SINR per user–BS per band. SINR is estimated for each user–BS link based on path loss models.
   - Blockage probability per user–BS per band. The blockage probability is obtained from the respective environment models (indoor, urban, and rural), accounting for materials, density etc. RF does not consider blockage, so its probability is zero for all BSs.

   The blockage model would contain information about the types of blockages in the environment (e.g., buildings), their positions and dimensions. Our function returns the blockage probability calculated based on the positions and the blockage model. We considered the urban environment in our model, so we used ray tracing. The urban model contains:
   - A 3D map of buildings in the urban environment.
   - Total number of rays to trace.

   It uses ray tracing to simulate signal propagation. The ray trace function traces the number of rays from the given position towards the surrounding buildings

represented in the urban map. It returns the number of rays "hits" that intersect with buildings.
The blockage probability is then calculated as the number of hits over the number of rays. This estimates the probability based on the fraction of rays that encounter a building during propagation.

- Normalize SINR across bands. SINR values are normalized to a 0–1 scale to make them comparable across frequency bands with different intrinsic path loss.

4. Calculate the blockage risk per band. Blockage risk is calculated as (1− Blockage Probability) to quantify the likelihood of an unblocked link. Higher values mean lower risk.
5. Calculate user scores per BS:
The proposed dynamic user association algorithm periodically calculates the association scores for each user–BS pair. The scores are based on real-time measurements.
User association scores are computed as the normalized SINR divided by (Blockage Risk + Category Weights). This balances the SINR, blockage effect, and user preferences differently for each band.

   - Score = NormSINR/(BlockageRisk + ProfileWeight).

   Let S_uk represent the association score between user u and BS k.
   The score is computed as a weighted sum of the SINR and blockage probability terms:

$$S_uk = w_1 * SINR + w_2 * B_{mm} \tag{22}$$

   - Higher weight given to preferred band based on user profile.
   User categories (e.g., high data rate, low latency, and high reliability) inform the weighting of blockage risk vs. SINR in scores. Higher weights prioritize users sensitive to that metric.
     - The 'highData' category is assigned a weight of 0.8.
     - The 'lowLatency' category is assigned a weight of 0.6.
     - The 'reliability' category (default/else case) is assigned a weight of 0.4.
   - Scores balance link metrics, blockage risk and user priorities.

   Figure 1 shows snapshot plots of the user scores for the three bands for several user profiles. This pattern suggests that there are distinct clusters or groups of users with different levels of performance or satisfaction. Some users are experiencing very poor performance or low satisfaction. These users may have low signal quality, high blockage probabilities, or other factors that lead to low user scores. Distribution does not significantly change between bands, which suggests load balancing among bands.
6. Rank the top BSs for each user by score.
7. Reassociate users in batches: Scores are periodically recomputed based on changing channel conditions. Users are reassigned to the best BSs in batches to gradually optimize the associations over time (based on time-varying scores).

   - Rank the top BSs for each user by score.
   - Select the BS from the top ranks weighted by scores.
   - Maintain the minimum users per band.

8. Monitor the network over time:

   - Track the SINR and throughput per user.
   - Update the blockage models and user profiles (categories) periodically.

9. Balance the BS loads if needed:

   - Transfer users from overloaded to underloaded BSs.

10. Repeat periodic reassociations:

    - Recompute the network state.

- Gradually reduce the preferred band weights.

11. Output and analyze:
    - User distributions per band.
    - Load balancing metrics.
    - Data rates and satisfaction levels.

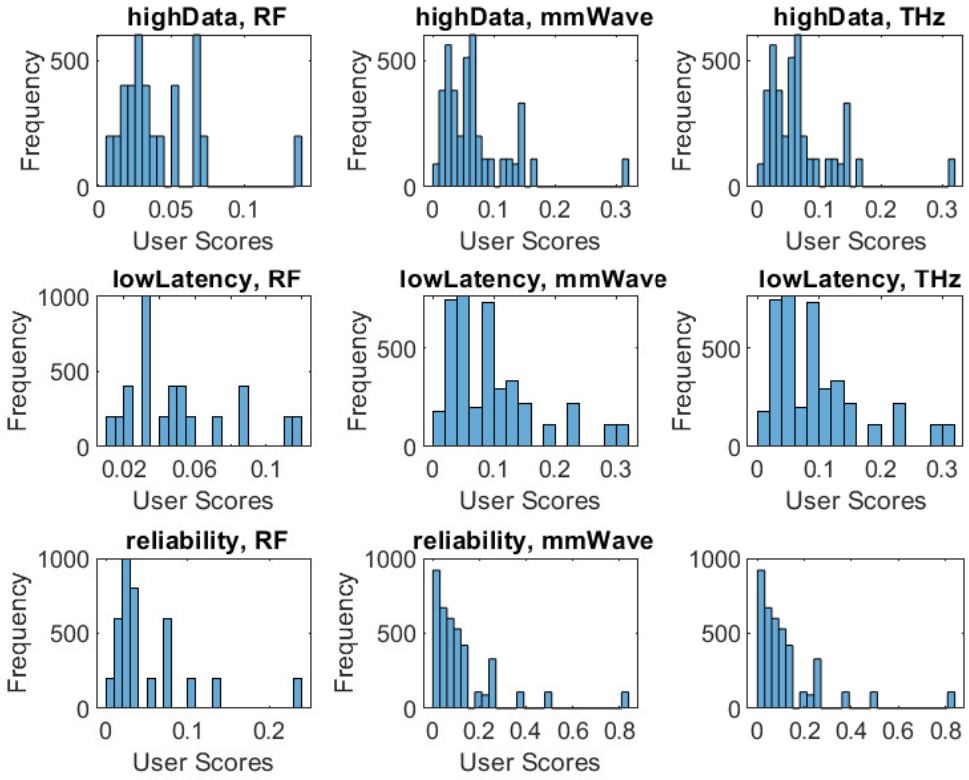

Figure 1. Scores illustration.

6. Results

Matlab^{TM} software (version MatlabR2023b) is used to analyze the performance of our proposed model. Monte Carlo simulations are run to estimate the coverage probability for different SINR thresholds, and an analytical solution for coverage probability is also derived.

Matlab simulation is performed to evaluate the performance of the proposed user association Algorithm 1. Table 2 lists the values we use in estimating the performance of the proposed method. Using 900 MHz to represent the sub-6 GHz RF band would be more appropriate than 2.4 GHz, given real-world deployments.

Here are some details on Canadian spectrum allocations for RF:

- In Canada and other countries, 900 MHz falls within the mainstream cellular allocations. Instead, 2.4 GHz is used mostly for unlicensed WiFi, so it does not represent the licensed cellular spectrum in the same way.
- The 700 MHz band (698–806 MHz) was auctioned off for commercial use and is being deployed for LTE.
- Cellular networks traditionally used the 800–900 MHz Extended Range CDMA (ER-CDMA) block, now being reframed for LTE.
- Bell Mobility and Telus operate terrestrial digital PCS networks in the 850–900 MHz bands.
- The 900 MHz band (806–960 MHz) is allocated for cellular and PMR use. It is commonly used by GSM networks.

The Microwave system models interference-limited coverage probability at a frequency of 900 MHz. Interferers are distributed according to a PPP. The user is interested in

achieving a target SINR threshold. Monte Carlo simulations are run to determine the coverage probability.

Algorithm 1 Multi-band user association algorithm.

Initialize: numUsers, numBS, userProfiles, BSbands, blockageModels, userPositions, BSpositions, associations
Categorize Users:
Categorize each user based on profile
Calculate Time-Varying Band Metrics:
Calculate raw SINR.
Calculate blockage Prob.
Normalize SINR across bands
Calculate Blockage Risk:
Calculate blockage risk per band
Calculate User Scores:
for each user i **do**
  for each BS j **do**
    score[i][j] = normalizeSINR[i][j]/(blockageRisk[j] + profileWeight[i][j])
  end for
end for
Reassociate Users:
for each batch of users **do**
  Rank BSs for each user by score
  Select BS weighted by scores
  Maintain min. Users Per Band
end for
Monitor Network:
Periodically track metrics
Update models and profiles
Balance Loads:
Transfer users between overloaded/underloaded BSs
Repeat re-associations periodically
Output results

Table 2. Simulation parameters.

Parameter	Value
Absorption coefficient	0.01 dB/km
Area Length	2000 m
Ref Distance	50 m
Density of interferers	0.00005 /m^2
Density of blockages	4×10^6 /m^2
blockage Len.	500 m
User Power	1 Watt
Transmitted power for RF	40 dBm
Transmitted power for mmW	30 dBm
Transmitted power for THz	10 dBm
Freq. RF	900 MHz
Freq. mmW	28 GHz
Freq. THz	1 THz
Number of Monte Carlo iterations	50

The interference power is modeled as a lognormal random variable, and the coverage probability is calculated analytically using the CDF of the interference power distribution. The results show which interference power distribution provides the closest match to the simulations.

The millimeter wave system consists of base stations, interferers, and blockages (modeled as rectangles), which are distributed according to a PPP. In our blockage model, first

we define the expected length and width of blockages and the number of blockages in the network area. We generate random blockage coordinates, then we check if a link is blocked by any of the blockages. If a link is blocked, then the path loss exponent is set to PL_{NLOS}, and the received signal strength is set to 0, modeling the complete blockage, and the interference from that interferer is also set to 0. If a link is not blocked, then the path loss exponent is set toPL_{LOS}, and the received signal and interference are calculated normally based on the distance, fading gains, and antenna gains.

THz wireless communication system is modeled using molecular absorption loss and exponential path loss. Also, system losses (L) are defined. The total noise consists of thermal noise and molecular noise.

This simulation models a wireless network with multiple base stations supporting different frequency bands, including RF, mmW and THz.

Users are distributed in the network area and can associate with different base stations based on the radio link quality and blockage risk. Environmental factors like propagation loss, blockage from walls, buildings, etc., are modeled to realistically capture how the signal strength (SINR) and link blockage probability vary across frequency bands and locations. The algorithm periodically evaluates SINR and blockage models to compute the association scores for each user–BS pair. It then reassociates users in batches to balance loads while considering each user's data needs and preferred band based on their category (e.g., high data and low latency). Network metrics like throughput and satisfaction levels are monitored over time as environmental conditions and user profiles dynamically change. This provides an end-to-end simulation of the multi-band user association approach to validate its effectiveness under realistic radio channel and deployment scenarios. The methodology considers changes to the network topology and BSs deployments over the simulated time period. The environment and network configuration are not static—they evolve dynamically as part of the long-term simulation.

The algorithm periodically re-evaluates user associations and network metrics, as both the environmental/user conditions and underlying network topology/deployments change and adapt over time.

As an example to clarify the UE profile change, UE profiles change with respect to latency/reliability requirements during the simulation. Each user is classified/categorized based on their expected data usage and priority needs. For example, some users may be considered "low latency critical" like VoLTE, while others are "high data" like video streaming. These categories define the user's preferred network characteristics—i.e., low-latency users want fast response times above all. However, a user's real-time needs are not static—a video caller may sometimes prioritize latency over reliability. To model this, each user's profile is associated with a time-varying probability distribution. For instance, a user has an 80 percent chance of being "low latency" but 20 percent of being "high reliability" at any given instant. When user profiles are updated, these probabilities are sampled to randomly switch users between categories. This simulates how priorities may change—a gaming user may occasionally download large files. The algorithm then adapts user associations accordingly to meet altered performance demands, capturing a more realistic scenario than that based on fixed assumptions about each user.

Figure 2 shows a comparison of load distribution for the proposed user association algorithm with max-SINR. For RF bands (sub-6 GHz), the number of users could range from a few hundred to over 1000 users within a 2000 m $\times$ 2000 m area depending on traffic levels. The number of base stations of usually 1–4 BSs would be needed to provide coverage within this area. For mmW bands (24–100 GHz), due to higher path loss, smaller cell sizes are needed (100 s of meters). The number of users could range from 50 to 200 within a single base station coverage area of 2000 m $\times$ 2000 m. The number of base stations is a very large number, 10–30, which would be needed within this area to provide coverage due to the small cell sizes needed. For THz bands (>100 GHz), cell sizes are expected to be tens of meters or less. The number of users is typically 1–10 users within a single base

station coverage area. The number of base stations is an extremely large number, 50–100, which would likely be needed within a 2000 m × 2000 m area to provide coverage.

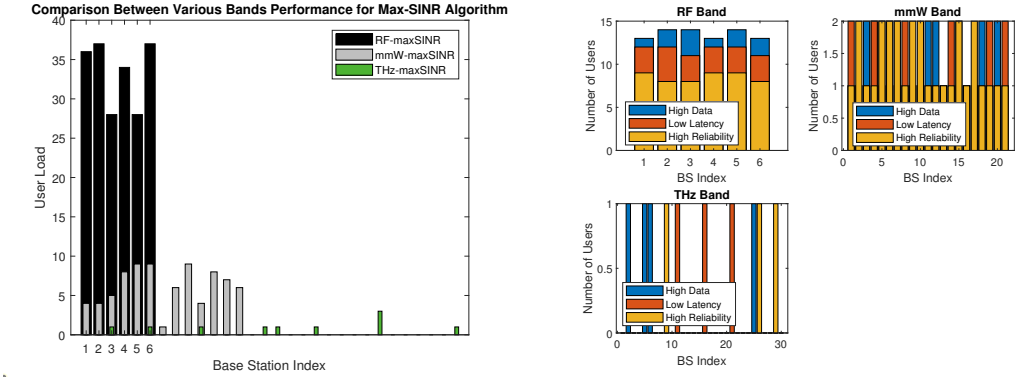

(**a**) (**b**)

Figure 2. User association comparison. (**a**) max-SINR for three bands. (**b**) Proposed algorithm for three bands.

We consider a network with 200 RF UEs and 6 RF BSs, 80 mmW UEs and 21 mmW BSs, and for THz 10 UEs and 30 BSs. The network has 80 high-data users, 70 low-latency users, and 50 high-reliability users for RF; 30 high-data users, 20 low-latency users, and 30 high-reliability users for mmW; and 4 high-data users, 3 low-latency users, and 3 high-reliability users for THz.

The results demonstrate that our algorithm associates users more effectively than the performance of max-SINR (this is evaluated by comparing standard deviation) balances the load across BSs, including those with lower transmit power that are underutilized by traditional approaches. Our proposed algorithm maintained an average standard deviation around 0.5 for the RF and mmW bands and 0.3 for THz band, unlike max-SINR, which has a standard deviation of 6.3456 for RF, 2.1543 for mmW, and 0.6972 for THz for all user categories as shown in Figure 2a,b. It is worth mentioning that max-SINR may show an acceptable performance in the THz band, but this is only because the number of users is much fewer than the number of BSs, so most of the distribution will be zeros, except for the associated ones, and this keeps the standard deviation low.

However, that is not the only issue, as the figures are only considering independent frequency bands assuming three independent networks, and each one is operating in a separate band.

When we evaluated an integrated network of RF, mmW, and THz BSs and UEs working together (a coexisting network of RF/mmW/THz), we concluded that any UE association algorithm, not just max-SINR that relies on SINR values or even the blockage score like many proposed methods in the literature, will fail in 6G coexisting networks. SINR for RF is the maximum value, which skews the results towards SINR RF after a certain point. No users are associated with the mmW or THz BSs. On the other hand, our algorithm still works well and provides a fair load distribution despite the wide spectrum of SINR values.

Figure 3 shows the SINR distribution plot and visualizes how SINR values are distributed across all users in each frequency band. The SINR distribution plot provides valuable insights into the quality of the wireless communication links between the users and the base stations in each frequency band.

The y-axis values indicate the count of occurrences of a particular SINR range in the histogram plot. This count is not directly related to the total number of users in the system. The count represents how many data points (in this case, SINR values) fall within each specified bin (SINR range) on the x-axis.

The histogram is constructed using the SINR values of users across the entire system, and it is possible for multiple users to have similar or the same SINR values, leading to multiple counts in the same SINR range.

max-SINR has a skewed distribution as in Figure 3a, which suggests that some users experience much better SINR than others, indicating an uneven user experience.

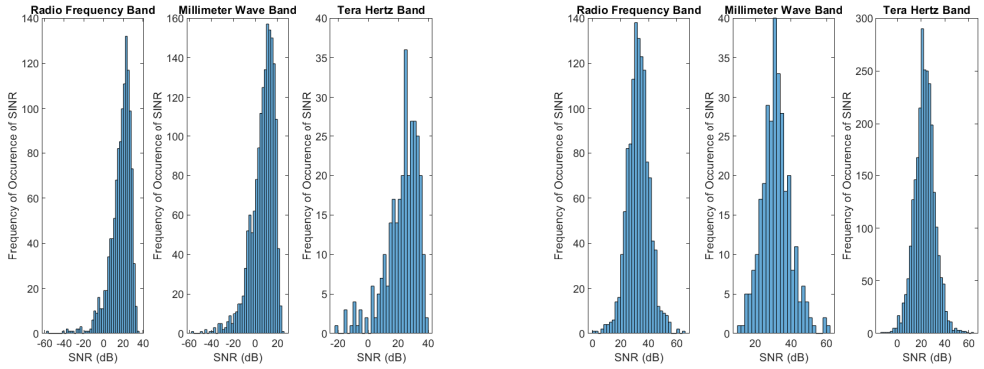

Figure 3. SINR distribution comparison for the three bands. (**a**) max-SINR algorithm. (**b**) Proposed algorithm.

As shown in Figure 3b, our proposed algorithm has a bell-shaped distribution, which indicates that most users experience SINR values around a certain central value, indicating good overall performance.

Figure 4 shows a comparison between the SINR coverage probability of three users (RF, millimeter, and THz users) in our network as a function of the SINR threshold for our proposed user association algorithm. THz and mmW bands can offer higher data rates and capacity due to their wider bandwidths, but their coverage distance may be limited due to higher path loss and attenuation. MW bands may provide more extended coverage distances and better penetration through obstacles but with comparatively lower data rates and capacity. The detailed reasons behind this are that at higher frequencies, the free space path loss increases significantly due to the shorter wavelengths. This results in higher signal attenuation and worse coverage. In addition, at frequencies above 100 GHz, molecular absorption due to oxygen, water vapor, and other gases starts to become significant. This leads to additional signal attenuation and reduces the coverage area. This effect is most prominent in the THz band. Higher-frequency signals have more difficulty penetrating common solid materials like walls, windows, foliage, etc. This results in more blockages and reduced coverage probability. This effect worsens with increasing frequency. Furthermore, to compensate for the higher path loss, transmitters at higher frequencies tend to use more directional antennas with narrower beamwidths. This reduces the coverage area of each transmitter. Simulation results follow the analytical solution.

Figure 5 shows the normalized throughput comparison (high data, low latency, and reliability) across the three bands (RF, mmW, and THz). High-data users prioritize high data rates, so they require more throughput to support their demands. However, the system may allocate resources preferentially to users with less stringent throughput needs like low latency and reliability. This could explain why high-data users see the lowest relative throughput.

Low-latency users have tight latency constraints that the network aims to satisfy, potentially at the expense of maximizing throughput. Their intermediate values suggest that resources are balanced between latency and throughput goals.

Reliability users are the most tolerant of throughput fluctuations. The system can prioritize their connections to maintain service quality. This likely leads to reliability users achieving the highest normalized throughput.

The RF band provides the least available bandwidth, limiting maximum the achievable throughput. mmW offers a bandwidth improvement but is more prone to blockage effects. THz has the highest bandwidth to maximize throughput, though it may face greater atmospheric attenuation challenges.

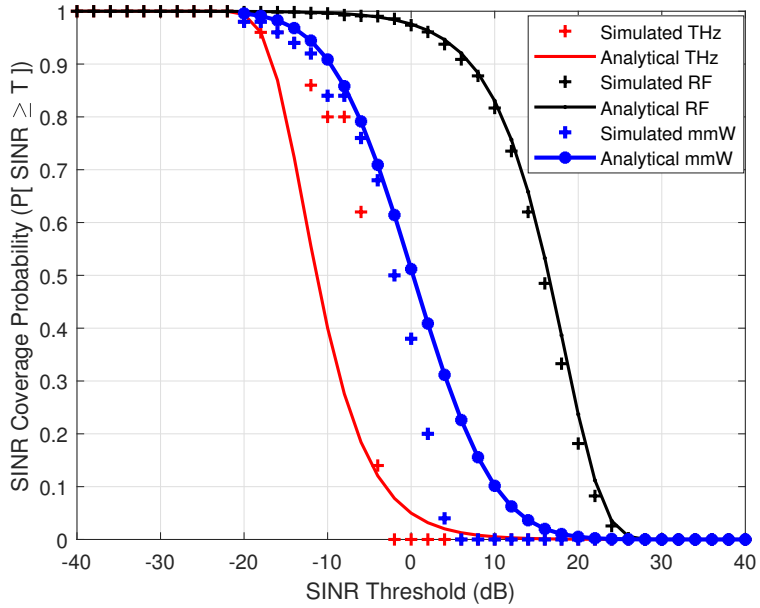

Figure 4. Coverage probability comparison.

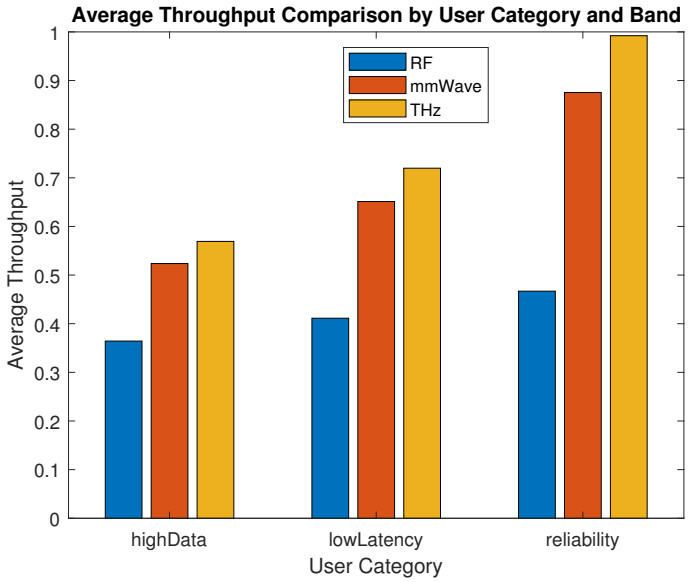

Figure 5. Throughput for the three bands by category.

Together, the user category priorities and band characteristics provide context for the observed trends of relatively lower throughput for high-data users sensitive to resource allocation, intermediate values for latency-focused associations, and the highest ones for reliability optimized connections across bands with increasing spectrum resources.

7. Conclusions

Multi-band solutions from RF to THz will play an important role in beyond 5G networks. However, optimized network planning, resource management and user association across multiple bands are needed to harness their full potential while mitigating the impact of higher propagation losses and interference at mmWave and THz frequencies.

We presented a novel dynamic user association algorithm for optimizing load balancing in integrated RF/mmWave/THz cellular networks. The algorithm periodically evaluates channel conditions and blockage risks across multiple frequency bands to calculate association scores for each user–BS pair. By factoring in user priorities and network

load metrics, it aims to reassociate users in a balanced way that optimizes overall resource utilization and QoE.

The simulation results demonstrate the algorithm's ability to efficiently utilize network resources across diverse channel conditions that vary with frequency. It provides an effective way to harness the advantages of multiple spectrum bands while mitigating their intrinsic propagation trade-offs. The algorithm achieves more balanced load distribution compared to traditional max-SINR approaches, while avoiding bias towards lower frequency bands.

The results also show that higher-frequency bands can offer advantages in terms of capacity and data rates, while lower-frequency bands provide better coverage. The choice of the optimal frequency band thus depends on specific application requirements, environment factors and performance trade-offs.

Future work includes extending the model to capture beamforming and directional communication effects at higher frequencies. Experimental validation on a multi-band prototype system would provide further validation of the approach. Overall, dynamic user association algorithms present a promising solution for realizing the full potential of multi-spectrum 5G and beyond networks.

Author Contributions: Conceptualization, N.H. and X.F.; methodology, N.H.; software, N.H.; validation, N.H., X.F. and I.W.; formal analysis, N.H.; investigation, N.H., X.F. and I.W.; resources, N.H.; data curation, N.H.; writing—original draft preparation, N.H.; writing—review and editing, N.H., X.F., I.W. and A.A.; visualization, X.F.; supervision, X.F. and I.W.; project administration, X.F.; funding acquisition, I.W. All authors have read and agreed to the published version of the manuscript.

Funding: This work has been supported by the Toronto Metropolitan University Faculty of Science Dean's Research Fund, and the NSERC Discovery Grant (REF #: RGPIN-2022-03798) held by the 3rd author.

Data Availability Statement: Data are contained within the article.

Acknowledgments: Authors would like to acknowledge the Dean of the Faculty of Science, TMU.

Conflicts of Interest: The authors declare no conflicts of interest.

Abbreviations

mmW	Millimeter wave
RF	Radio frequency
6G	Sixth generation
LOS	Line of sight
NLOS	Non-line of sight
SINR	Signal-to-interference and noise ratio
SNR	Signal-to-noise ratio
MIMO	Multiple input multiple output
BS	Base station
UE	User equipment
QoS	Quality of service
QoE	Quality of experience
CRE	Cell range expansion
eICIC	Enhanced intercell interference coordination
PPP	Poisson point process
OFCDM	Orthogonal frequency and code division multiplexing
OFDM	Orthogonal frequency division multiplexing
RAT	Radio access technology

References

1. Kato, N.; Mao, B.; Tang, F.; Kawamoto, Y.; Liu, J. Ten challenges in advancing machine learning technologies toward 6G. *IEEE Wirel. Commun.* **2020**, *27*, 96–103. [CrossRef]

2. Letaief, K.B.; Shi, Y.; Lu, J.; Lu, J. Edge artificial intelligence for 6G: Vision, enabling technologies, and applications. *IEEE J. Sel. Areas Commun.* **2021**, *40*, 5–36. [CrossRef]
3. Khan, M.Q.; Gaber, A.; Schulz, P.; Fettweis, G. Machine Learning for Millimeter Wave and Terahertz Beam Management: A Survey and Open Challenges. *IEEE Access* **2023**, *11*, 11880–11902. [CrossRef]
4. Fascista, A.; De Monte, A.; Coluccia, A.; Wymeersch, H.; Seco-Granados, G. Low-complexity downlink channel estimation in mmwave multiple-input single-output systems. *IEEE Wirel. Commun. Lett.* **2021**, *11*, 518–522. [CrossRef]
5. Sarieddeen, H.; Saeed, N.; Al-Naffouri, T.Y.; Alouini, M.S. Next generation terahertz communications: A rendezvous of sensing, imaging, and localization. *IEEE Commun. Mag.* **2020**, *58*, 69–75. [CrossRef]
6. Mallat, N.K.; Ishtiaq, M.; Ur Rehman, A.; Iqbal, A. Millimeter-wave in the face of 5G communication potential applications. *IETE J. Res.* **2022**, *68*, 2522–2530. [CrossRef]
7. Nagatsuma, T. Terahertz technologies: Present and future. *IEICE Electron. Express* **2011**, *8*, 1127–1142. [CrossRef]
8. Han, C.; Wang, Y.; Li, Y.; Chen, Y.; Abbasi, N.A.; Kürner, T.; Molisch, A.F. Terahertz wireless channels: A holistic survey on measurement, modeling, and analysis. *IEEE Commun. Surv. Tutor.* **2022**, *24*, 1670–1707. [CrossRef]
9. Akyildiz, I.F.; Han, C.; Hu, Z.; Nie, S.; Jornet, J.M. Terahertz band communication: An old problem revisited and research directions for the next decade. *IEEE Trans. Commun.* **2022**, *70*, 4250–4285. [CrossRef]
10. Wang, C.X.; You, X.; Gao, X.; Zhu, X.; Li, Z.; Zhang, C.; Wang, H.; Huang, Y.; Chen, Y.; Haas, H.; et al. On the road to 6G: Visions, requirements, key technologies and testbeds. *IEEE Commun. Surv. Tutor.* **2023**, *25*, 905–974. [CrossRef]
11. Hakeem, S.A.A.; Hussein, H.H.; Kim, H. Vision and research directions of 6G technologies and applications. *J. King Saud Univ. Comput. Inf. Sci.* **2022**, *34*, 2419–2442.
12. Abdel Hakeem, S.A.; Hussein, H.H.; Kim, H. Security requirements and challenges of 6G technologies and applications. *Sensors* **2022**, *22*, 1969. [CrossRef] [PubMed]
13. Sopin, E.; Moltchanov, D.; Daraseliya, A.; Koucheryavy, Y.; Gaidamaka, Y. User association and multi-connectivity strategies in joint terahertz and millimeter wave 6G systems. *IEEE Trans. Veh. Technol.* **2022**, *71*, 12765–12781. [CrossRef]
14. Wang, L.; Ai, B.; Niu, Y.; Jiang, H.; Mao, S.; Zhong, Z.; Wang, N. Joint User Association and Transmission Scheduling in Integrated mmWave Access and Terahertz Backhaul Networks. *IEEE Trans. Veh. Technol.* 2023, *early access*. [CrossRef]
15. Altman, E.; Kumar, A.; Singh, C.; Sundaresan, R. Spatial SINR games of base station placement and mobile association. *IEEE/ACM Trans. Netw.* **2012**, *20*, 1856–1869. [CrossRef]
16. Dhungana, Y.; Tellambura, C. Multichannel analysis of cell range expansion and resource partitioning in two-tier heterogeneous cellular networks. *IEEE Trans. Wirel. Commun.* **2015**, *15*, 2394–2406. [CrossRef]
17. Kong, F.; Sun, X.; Leung, V.C.; Zhu, H. Delay-optimal biased user association in heterogeneous networks. *IEEE Trans. Veh. Technol.* **2017**, *66*, 7360–7371. [CrossRef]
18. Deb, S.; Monogioudis, P.; Miernik, J.; Seymour, J.P. Algorithms for enhanced inter-cell interference coordination (eICIC) in LTE HetNets. *IEEE/ACM Trans. Netw.* **2013**, *22*, 137–150. [CrossRef]
19. Nie, X.; Wang, Y.; Zhang, J.; Ding, L. Coverage and Association Bias Analysis for Backhaul Constrained HetNets with eICIC and CRE. *Wirel. Pers. Commun.* **2017**, *97*, 4981–5002. [CrossRef]
20. Hassan, N.; Fernando, X. Interference mitigation and dynamic user association for load balancing in heterogeneous networks. *IEEE Trans. Veh. Technol.* **2019**, *68*, 7578–7592. [CrossRef]
21. Hassan, N.; Fernando, X. An optimum user association algorithm in heterogeneous 5G networks using standard deviation of the load. *Electronics* **2020**, *9*, 1495. [CrossRef]
22. Zarifneshat, M.; Roy, P.; Xiao, L. Multi-objective approach for user association to improve load balancing and blockage in millimeter wave cellular networks. *IEEE Trans. Mob. Comput.* **2021**, *22*, 2818–2836. [CrossRef]
23. Chen, Q.; Chen, H.; Chai, R.; Zhao, D. Network utility optimization-based joint user association and content placement in heterogeneous networks. *EURASIP J. Wirel. Commun. Netw.* **2018**, *2018*, 122. [CrossRef]
24. Achki, S.; Aziz, L.; Gharnati, F.; Ait Ouahman, A. User association strategy for energy efficiency and interference mitigation of heterogeneous networks. *Adv. Mater. Sci. Eng.* **2020**, *2020*, 7018727. [CrossRef]
25. Selvi, M.P.; Shobanadevi, N. An efficient artificial rabbits optimization-based user association problems in ultradense network using deep learning model. *Int. J. Commun. Syst.* **2023**, *36*.
26. Zhai, D.; Li, H.; Tang, X.; Zhang, R.; Cao, H. Joint position optimization, user association, and resource allocation for load balancing in UAV-assisted wireless networks. *Digit. Commun. Netw.* 2022, *in press*. [CrossRef]
27. Jain, A.; Lopez-Aguilera, E.; Demirkol, I. User association and resource allocation in 5G (AURA-5G): A joint optimization framework. *Comput. Netw.* **2021**, *192*, 108063. [CrossRef]
28. Siddiqui, A.B.; Aqeel, I.; Alkhayyat, A.; Javed, U.; Kaleem, Z. Prioritized user association for sum-rate maximization in UAV-assisted emergency communication: A reinforcement learning approach. *Drones* **2022**, *6*, 45. [CrossRef]
29. Bai, W.; Wang, Y. Jointly Optimize Partial Computation Offloading and Resource Allocation in Cloud-Fog Cooperative Networks. *Electronics* **2023**, *12*, 3224. [CrossRef]
30. Chen, C.; Niu, Y.; Mao, S.; Zhang, X.; Han, Z.; Ai, B.; Gao, M.; Xiao, H.; Wang, N. Coalition game based user association for mmWave mobile relay systems in rail traffic scenarios. *IEEE Trans. Veh. Technol.* **2021**, *70*, 10528–10540. [CrossRef]
31. Alizadeh, A.; Vu, M. Distributed user association in B5G networks using early acceptance matching game. *IEEE Trans. Wirel. Commun.* **2020**, *20*, 2428–2441. [CrossRef]

32. Li, Z.; Wang, C.; Jiang, C.J. User association for load balancing in vehicular networks: An online reinforcement learning approach. *IEEE Trans. Intell. Transp. Syst.* **2017**, *18*, 2217–2228. [CrossRef]
33. Zhao, N.; Liang, Y.C.; Niyato, D.; Pei, Y.; Wu, M.; Jiang, Y. Deep reinforcement learning for user association and resource allocation in heterogeneous cellular networks. *IEEE Trans. Wirel. Commun.* **2019**, *18*, 5141–5152. [CrossRef]
34. Wang, L.; Wang, K.; Pan, C.; Xu, W.; Aslam, N.; Nallanathan, A. Deep reinforcement learning based dynamic trajectory control for UAV-assisted mobile edge computing. *IEEE Trans. Mob. Comput.* **2021**, *21*, 3536–3550. [CrossRef]
35. Chen, C.; Zhang, J.; Chu, X.; Zhang, J. On the optimal base-station height in mmWave small-cell networks considering cylindrical blockage effects. *IEEE Trans. Veh. Technol.* **2021**, *70*, 9588–9592. [CrossRef]
36. Rahimian, A.; Mehran, F. RF link budget analysis in urban propagation Microcell environment for mobile radio communication systems link planning. In Proceedings of the Wireless Communications and Signal Processing (WCSP), Nanjing, China, 9–11 November 2011; pp. 1–5.
37. Rao, K.D.; Rao, K.D. Overview of the Performance of Digital Communication Over Fading Channels. *Channel Coding Tech. Wirel. Commun.* **2019**, 23–53.
38. Ayidu, N.J.; Elaigwu, V. Pathloss prediction model in wlan propagation. *Fudma J. Sci.* **2023**, *7*, 1–5. [CrossRef]
39. XING, B.q.; WEI, Z.x. Time-Varying Channel Modeling and Simulation Based on 3GPP TR38. 901 Channel Model. *J. Beijing Univ. Posts Telecommun.* **2021**, *44*, 45.
40. Elayan, H.; Shubair, R.M.; Jornet, J.M. Characterising THz propagation and intrabody thermal absorption in iWNSNs. *IET Microwaves Antennas Propag.* **2018**, *12*, 525–532. [CrossRef]
41. Hesham, E.; Gadelrab, M.S.; ElSayed, K.; Sallam, A.R. Modelling Multilayer Communication Channel in Terahertz Band for Medical Applications. *Int. J. Commun. Netw. Inf. Secur.* **2021**, *13*, 358–365.
42. Sayehvand, J.; Tabassum, H. Interference and coverage analysis in coexisting RF and dense terahertz wireless networks. *IEEE Wirel. Commun. Lett.* **2020**, *9*, 1738–1742. [CrossRef]
43. Petrov, V.; Komarov, M.; Moltchanov, D.; Jornet, J.M.; Koucheryavy, Y. Interference and SINR in millimeter wave and terahertz communication systems with blocking and directional antennas. *IEEE Trans. Wirel. Commun.* **2017**, *16*, 1791–1808. [CrossRef]
44. Wang, Y.; Chen, C.; Chu, X. Performance Analysis for Hybrid mmWave and THz Networks with Downlink and Uplink Decoupled Cell Association. *arXiv* **2023**, arXiv:2308.05842.
45. Piesiewicz, R.; Jansen, C.; Mittleman, D.; Kleine-Ostmann, T.; Koch, M.; Kurner, T. Scattering analysis for the modeling of THz communication systems. *IEEE Trans. Antennas Propag.* **2007**, *55*, 3002–3009. [CrossRef]